Engineered Science

RESEARCH PAPER

View Article Online

pH and Electromagnetic Dual-Remoted Drug Delivery Based on Bimodal Superparamagnetic Fe_3O_4@Porous Silica Nanoparticles

Haihua Hu,[1,2] Haopeng Liu,[1,2] Dianjun Zhang,[1,2] Jianjun Wang,[3] Gaowu Qin[3] and Xuefeng Zhang*[1,2]

We developed a molecular-grafting procedure to the synthesis of ultrathin Fe_3O_4 decorated Fe_3O_4/silica core/shell nanoparticles. Such nanoparticles demonstrated superparamagnetic transitions at temperatures of 14 K and 213 K and weak magnetic interactions between the decorated ultrathin Fe_3O_4 and Fe_3O_4 cores. When evaluated for the electromagnetically/pH switchable drug delivery, the Fe_3O_4/silica/Fe_3O_4 nanoparticles manifest a better controllability for enhancing the drug release than the Fe_3O_4/silica nanoparticles, ascribed to the bimodal hyperthermia effect of internal ~10 nm Fe_3O_4 cores and externally decorated ~2.5 nm Fe_3O_4 nanoparticles.

Keywords: Fe_3O_4; nanoparticles; superparamagnetic

Received 11th April 2018, Accepted 23rd April 2018

DOI: 10.30919/es8d136

1. Introduction

Targeted drug delivery triggered by various external stimulus such pH,[1–8] DNA,[9–12] enzyme[13–14] and photo,[15–17] have been attracting considerable interests due to their promising potential for many applications. Incorporation of magnetic matter into carriers that can be manipulated by external magnetic fields, in particular, have demonstrated the advantages for multi-functional use in the delivery/recovery, enzyme immobilization,[14] magnetic resonance imaging (MRI), and localized therapy such as hyperthermia. The advantage of ultrasound generated from magnetic fields is that the magnetic fields do not suffer the same attenuation as ultrasound through bones or soft tissue, and nanoparticles can be successfully delivered to various places in the human body.[18] Among the many examples reported so far,[19–29] Giri *et al.* have used Fe_3O_4 nanoparticles as magnetically-manipulated bars and blocking caps to control the release of fluorescein molecules.[21] Li *et al.* researched the hollow mesoporous silica nanoparticles with tunable structures for controlled drug delivery.[22] Zhu *et al.* reported the rattle-type Fe_3O_4/silica hollow mesoporous spheres for the loading and release of doxorubicin hydrochloride (DOX).[23] Kong *et al.* reported Fe_3O_4/silica nanoparticles for the anticancer drug delivery and the controlled on-off switchable release by remote electromagnetic field.[29]

In this work, we report a protocol to synthesize ultrathin Fe_3O_4 decorated Fe_3O_4/silica core/shell nanoparticles (hereafter denoted as Fe_3O_4/silica/u-Fe_3O_4), and their use to enhanced the efficacy for the electromagnetically controllable release of anticancer drug, doxorubicin (DOX), as shown in Figure 1. Doxorubicin is one of the most widely used anticancer drugs due to its promising potential against solid tumors. The therapy, however, is limited by dose-dependent toxic side effects which can potentially lead to heart failure due to cardiotoxicity. To overcome this problem, targeted drug delivery can provide therapeutically effective drug release directly at the tumor site to improve the treatment of cancers. The coupled doxorubicin molecules are immobilized with the amides to strongly inhibit the diffusion from the surface of nanoparticles, but they can be released at mild acid condition ascribed to the pH-clickable amide linkers.[5] When stimulated by an external electromagnetic field, the release of doxorubicin molecules exhibit an enhanced response ascribed to the co-operative hyperthermia effect of two kinds of superparamagnetic Fe_3O_4 core and decorated u-Fe_3O_4 nanoparticles, providing the possibility of dual-modal controllability of drug release dependent on pH and the external electromagnetic field.

2. Experimental section

2.1. Materials

All reagents used in this study are commercially available. Oleic acid (OA, 90%), 1-hexaneol anhydrous (99%), octyl ether (98%), ammonia solution (NH_4OH, 28-30 wt % in water), Triton X-100, hexane (95%), cylcohexane (99.5%), Dimethyl sulfoxide (DMSO, 99%), 1,2-cis-cyclohexanedicarboxylic anhydride (98%), Triethylamine (98%), tetraethoxysilane (TEOS, 99.999%), sodium hydroxide (99%), N,N-Dimethylformamide (DMF, 99.8%), tetrachloroaurate(III) hydrate

[1] *Key Laboratory for Anisotropy and Texture of Materials (ME), School of Materials Science and Engineering, Northeastern University, Shenyang 110819, PR China. E-mail: zhang@hdu.edu.cn*

[2] *Innovative Center of Advanced Materials, Hangzhou Dianzi University, Hangzhou 310018, PR China. E-mail: zhang@hdu.edu.cn*

[3] *Shenyang Northeastern Institute of Metal Materials Co., Ltd, Shenyang 110108, PR China*

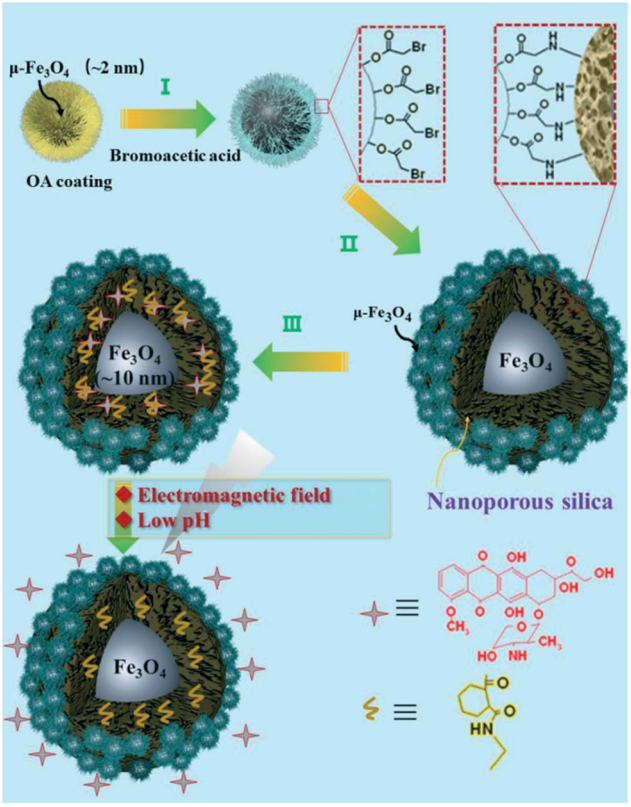

Fig. 1 Scheme of ultrathin Fe_3O_4 nanoparticles decorated Fe_3O_4/silica nanoparticles for DOX conjugation and release under external pH and electromagnetic field stimuli.

(99.99%), bromoacetic acid (97%) and Doxorubicin hydrochloride (98%) were purchased from Sigma-Aldrich Inc. Iron pentacarbonyl (99.5%) was purchased from Strem Chemicals, Inc. (Newburyport, MA) and N-(2-aminoethyl)-3-aminopropyltrimethoxysilane (AEAP3, ≥ 90%) was purchased from Gelest (Tullytown, PA).

2.2. Synthesis of core/shell Fe_3O_4/silica nanoparticles

The core/shell Fe_3O_4/silica nanoparticles were synthesized in a water-in-oil microemulsion that contains the oleic acid-coated Fe_3O_4 nanoparticles as seeds. 0.5 ml of 1 mg/mL Fe_3O_4/cyclohexane dispersion was injected into a mixture of 1.77 g of Triton X-100, 1.6 ml of anhydrous 1-hexanol and 7 ml of cyclohexane under a strong vortex for about 1 h. 0.5 ml of 6% ammonia solution was added and carried out the vortex for another 1 h, and then 25 μl of TEOS were added to allow the reaction for 24 h. Subsequently, 25 μl of AEAP3 were injected into the reaction mixture for another 24 h. The resultant product was core/shell structure Fe_3O_4/silica nanoparticles with nanoporous silica shells. The nanoparticles were centrifuged at 9000 rpm and washed with anhydrous ethanol three times, and finally dispersed in de-ionized water for usage.

2.3. Decoration of ultrathin Fe_3O_4 nanoparticles on the surface of Fe_3O_4/silica nanoparticles

Oleic acid-coated ultrathin Fe_3O_4 (u-Fe_3O_4) nanoparticles with a mean diameter of 2.5 nm were modified by bromoacetic acid and the detailed procedures is as that reported by Xu.[1] In the first step, 0.5 g of bromoacetic acid and 0.5 g of citric acid were dissolved in a mixture of 5 ml chloroform and 5 ml DMF. Subsequently, 10 mg 2.5 nm oleic acid-coated u-Fe_3O_4 nanoparticles were added, then sonicated for 1 hour and stirred for overnight at 30 °C to form stable dispersion. The surface-modified u-Fe_3O_4 nanoparticles were separated by centrifugation and washed for 3 times by 30 mL ethanol to remove excess bromoacetic acid. Finally, 5 mg Fe_3O_4/silica nanoparticles were mixed with surface-modified u-Fe_3O_4 nanoparticles in 5 mL ethanol, and stirred for overnight. The Fe_3O_4/silica/u-Fe_3O_4 nanoparticles were washed and centrifuged at 9000 rpm for 20 min, and dispersed in de-ionized water for usage.

2.4. Doxorubicin loading and pH-regulated release

2 mg Fe_3O_4/silica/u-Fe_3O_4 (or Fe_3O_4/silica) nanoparticles were dissolved in 20 mL DMSO, followed by sonicating for 30 min. Excess 1,2-cis-cyclohexanedicarboxylic anhydride was subsequently added and magnetically stirred for 2 h. The nanoparticles were separated by centrifuged at 9000 rpm, and mildly washed by DMSO for three times. The grafted nanoparticles and doxorubicin hydrochloride salt (1 mg) was dissolved in 20 mL DMSO solution with 100 μL triethylamine, and magnetically stirred for 6 h at room temperature. In order to remove the free doxorubicin molecules, the doxorubicin-coupled nanoparticles were separated by centrifuged and mildly washed by pH7.4 phosphoric acidic buffer solution for three times. The release of doxorubicin from coupled Fe_3O_4/silica/u-Fe_3O_4 nanoparticles was carried out at 37 °C and at pH 7.4 and 5.0 phosphoric acidic buffer solutions, respectively. The separated supernatant solution was monitored by UV-Vis spectra. Under the alternative electromagnetic field of the frequency of 400 kHz, the nanoparticles generate the hyperthermia effect to induce the temperature increase, and produce the DOX release. The temperature was measured by infrared thermometer (Fisher Scientific), and the post-released solution at each measured point was immediately centrifuged at 10 °C avoiding the furthermore release.

2.5. Characterization methods

The size and morphology of nanoparticles were analyzed using a Hitachi S-4700 transmission electron microscopy (TEM) operated at a voltage of 30 kV. Microstructure and composition of the samples were characterized by using a JEOL 2010F (200 kV) high resolution TEM (HRTEM). UV–Vis spectra were collected on a Perkin Elmer Lamda 950 spectrometer. Magnetic measurements of major hysteresis loops (MHL) at different temperatures as well as zero-field cooled (ZFC) magnetization processes were performed with a Quantum Design PPMS model 6000 magnetometer.

2.6. Cell viability measurements

DOX release and the cytotoxicity of the Fe_3O_4/silica(porous) core/shell nanoparticles functionalised with DOX were evaluated using adenocarcinomic human alveolar basal epithelial cells (A549, American Type Culture Collection (ATCC), USA). The medium used was Ham's F-12 (ATCC, USA) supplemented with penicillin (100 IU/mL), streptomycin (100 μg/mL) and 10% fetal bovine serum (FBS). The cells were cultured at a density of 1×10^5 cells per 1 mL of medium in 24-well culture plates at 37°C in a 5% CO_2 atmosphere. After 20 h of culture, the medium in the wells was replaced with fresh medium containing Fe_3O_4/silica(porous) core/shell nanoparticles (1, 5, 10 and 50 μg/mL),

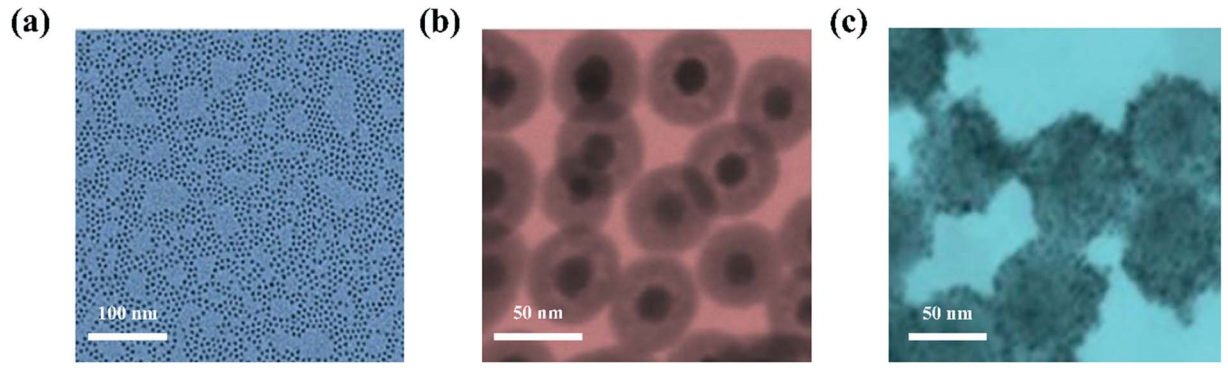

Fig. 2 TEM images of (a) ultrathin Fe_3O_4 nanoparticles; (b) Fe_3O_4/silica nanoparticles; (c) DOX conjugated Fe_3O_4/silica/u-Fe_3O_4 nanoparticles.

Fe_3O_4/silica(porous) core/shell nanoparticles functionalised with DOX (1, 5, 10 and 50 μg/mL) and DOX (0.1, 0.5 and 1, 5 μg/mL), and was further cultured for 48 h. In control cultures, the cells were placed in a medium without nanoparticles at the same cell density.

The cell viability test was carried out *via* the reduction of the MTT reagent (Invitrogen). After 48h of culture with the Fe_3O_4/silica(porous) core/shell nanoparticles (1, 5 and 10, 50 μg/mL), Fe_3O_4/silica(porous) core/shell nanoparticles functionalized with DOX (1, 5 and 10, 50 μg/mL) and free DOX (0.1, 0.5 and 1, 5 μg/mL), 100 μl of MTT dye solution (5 mg/ml in phosphate buffer pH-7.4) was added to each well and incubated for 4 h at 37°C and 5% CO_2. The medium was removed and formazan crystals were solubilized with 150 μl of dimethylsulphoxide (DMSO). Absorbance of each well was read using a spectrophotometer (Biotek, USA) at 540 nm and the relative cell viability (%) related to control wells containing cell culture medium without nanoparticles was calculated by $[A]_{test}/[A]_{control} \times 100$. Three replicates were measured, and the results presented as mean ± standard deviation.

3. Results and discussion

The experimental details of the synthesis of two kinds of Fe_3O_4 nanoparticles have been reported previously.[5] The Fe_3O_4/silica core/shell nanoparticles with terminus amine groups and nanoporous structures were synthesized by a water-in-oil microemulsion. 0.5 ml of 1 mg/mL Fe_3O_4 nanoparticles in cyclohexane was rapidly injected into a mixture of 1.77 g of Triton X-100, 1.6 ml of anhydrous 1-hexanol and 7 ml of cyclohexane under a strong vortex for 1 h., following the addition of 0.5 mL of ammonia solution (6 % ammonia solution) for 1 h. Subsequently, 10 μl TEOS and 10 μl AEAP3 were added in sequence to allow each step reaction for 24 h. The resultant product was centrifuged at 9000 rpm and washed with anhydrous ethanol three times, and dispersed in de-ionized water.

In the synthesis of Fe_3O_4/silica/u-Fe_3O_4 nanoparticles, the u-Fe_3O_4 nanoparticles with oleic acid stabilized surface were firstly functionalized by bromoacetic acid, forming the terminal bromine groups, which

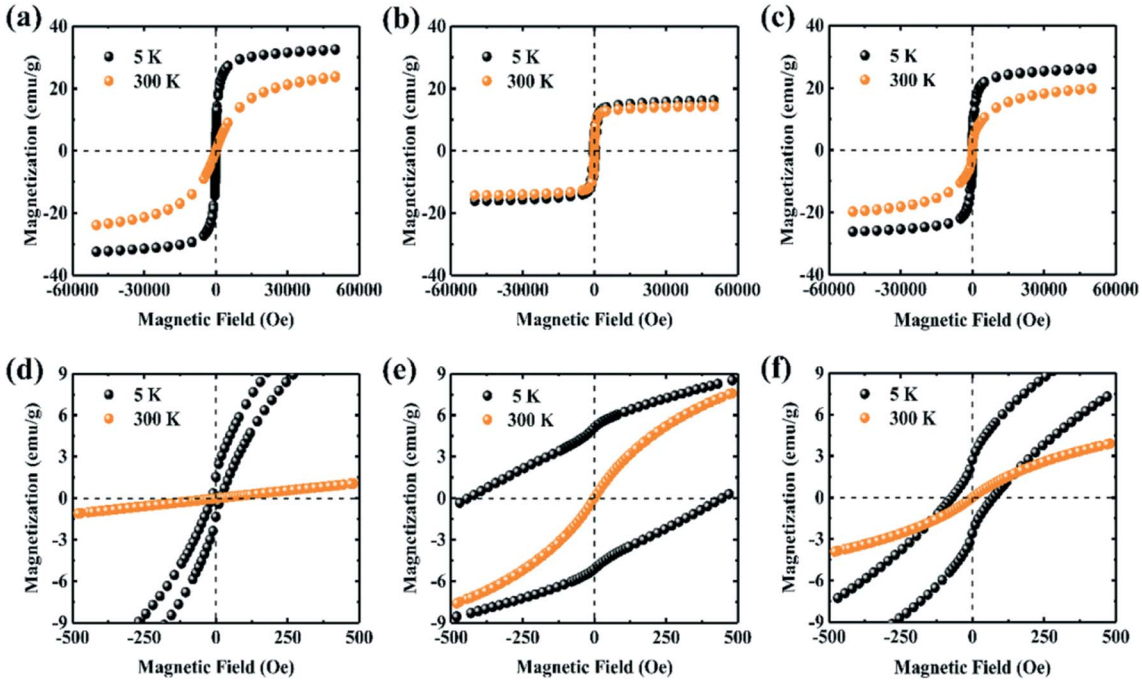

Fig. 3 Magnetic loops of (a) and (d) ultrathin Fe_3O_4 nanoparticles; (b) and (e) core/shell Fe_3O_4/silica nanoparticles; (c) and (f) DOX conjugated Fe_3O_4/silica/u-Fe_3O_4 nanoparticles.

further reacted with the amine groups of silica shell by nucleophilic substitution. The Fe_3O_4/silica/u-Fe_3O_4 nanoparticles were then functionalized by the chemical graft of 1,2-cyclohexanedicarboxylic anhydride as click linkers, and conjugated by doxorubicin molecules. The loading and release of DOX-Fe_3O_4/silica/u-Fe_3O_4 nanoparticles dispersed in PBS (5 or 7.4) were evaluated by on a Perkin Elmer Lamda 950 spectrometer by the absorption peak intensity at 504 nm. The alternative electromagnetic field generator was a self-made device with an output current of 40 A and voltages of 200 V and a frequency of 400 kHz. A centrifuge tube containing the nanoparticle suspension is placed at the center of the coil, and the temperature was in-situ measured by infrared thermometer (Fisher Scientific).

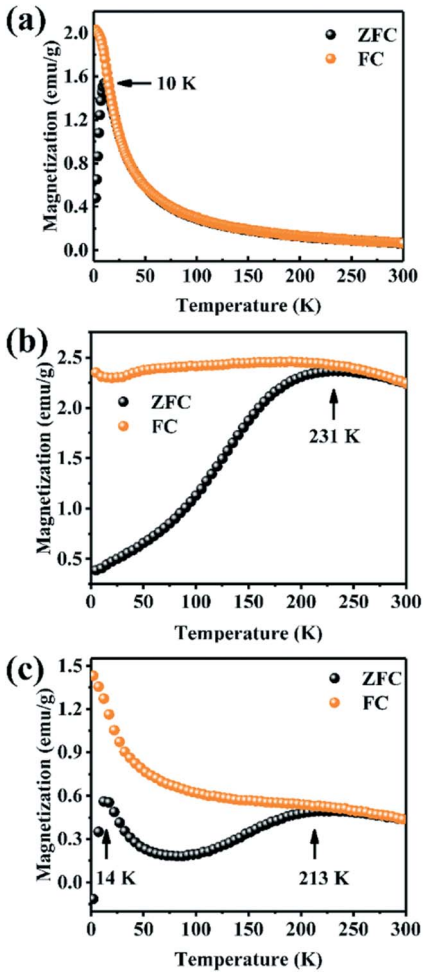

Fig. 4 ZFC-FC curves of (a) ultrathin Fe_3O_4 nanoparticles; (b) core/shell Fe_3O_4/silica nanoparticles; (c) DOX conjugated Fe_3O_4/silica/u-Fe_3O_4 nanoparticles.

Figure 2(a) shows transmission electron microscopy (TEM) image of both oleic acid stabilized Fe_3O_4 nanoparticles with a mean diameter of 2.5 nm (u-Fe_3O_4). Figure 2(b) and (c) show TEM images of the synthesized Fe_3O_4/silica core/shell nanoparticles and DOX-conjugated Fe_3O_4/silica/u-Fe_3O_4 nanoparticles, respectively. The silica shells of Fe_3O_4/silica core/shell nanoparticles were uniform with a mean thickness of 20 nm and nanoporous structure that extended to the outside surface. The nanoporous structure provides the loading capacity for the subsequent conjugation of DOX molecules in the inner pores of silica shells.[30–31] Following immobilization of the 2.5 nm Fe_3O_4 nanoparticles and DOX molecules, the nanoparticles observed in the TEM images still remain mono-dispersible. It is noted that the surface was slightly changed to be rough, probably induced by the chemical reaction in conjugation process. The DOX-conjugated Fe_3O_4/silica/u-Fe_3O_4 nanoparticles displayed typical characteristic peaks of doxorubicin molecules at 450~550 nm, implying that the u-Fe_3O_4 nanoparticles cannot arrest the diffusion of DOX molecules into the inner pores of silica shells.

Figure 3(a), (b) and (c) show the major hysteresis loops (MHLs) and corresponding enlargements of u-Fe_3O_4, Fe_3O_4/silica and Fe_3O_4/silica/u-Fe_3O_4 nanoparticles at 300 and 5 K. All the three nanoparticles exhibit typical superparamagnetic behavior, together with nearly zero coercive fields at room temperature. At 5 K, the MHLs present increased coercive fields (*Hc*) of 13, 445 and 70 Oe, and saturation magnetizations of 32, 16 and 26 emu/g. The low saturation magnetization of u-Fe_3O_4 nanoparticles is attributed to the thermal fluctuation and magnetically disordered surface.[32] Regardless of the loading of doxorubicin molecules, one can estimate the mass fractions of u-Fe_3O_4 and Fe_3O_4/silica nanoparticles are 62.5and 37.5 wt.%, respectively, based on the saturation magnetization values.

Figure 4(a), (b) and (c) show the temperature-dependent zero-field-cooling (ZFC) and field-cooling (FC) magnetization curves of u-Fe_3O_4, Fe_3O_4/silica and Fe_3O_4/silica/u-Fe_3O_4 nanoparticles, respectively, at an applied magnetic field of 50 Oe. The ZFC/FC curves of u-Fe_3O_4 nanoparticles exhibit a sharp cusp at 10 K, corresponding to the transition from ferromagnetic to superparamagnetic behavior. The transition temperature is defined as the blocking temperature (T_B). Below T_B, the magnetic moments are free; in other

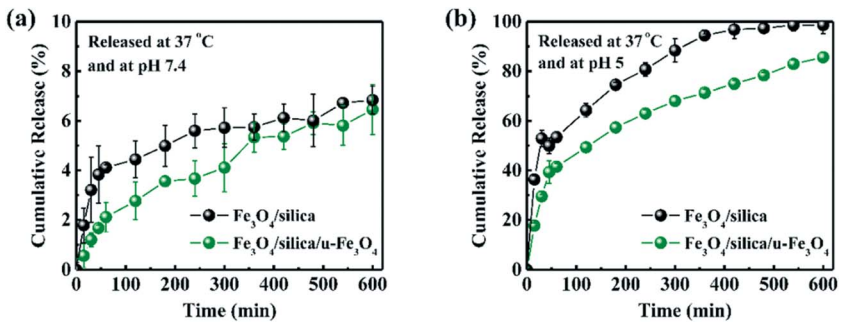

Fig. 5 DOX release curves of two kinds of nanoparticles, (a) 37 °C, pH 7.4; (b) 37 °C, pH 5.

words, they can freely relax during the time of the measurement. The transition in ZFC/FC curves of Fe_3O_4/silica nanoparticles shifts up to 231 K, showing that they are also superparamagnetic at room temperature. The different transition temperatures between u-Fe_3O_4 and Fe_3O_4/silica are mainly ascribed to the size effect, which are consistent with the particle size as observed from TEM images. Furthermore, the ZFC/FC curves of Fe_3O_4/silica/u-Fe_3O_4 nanoparticles exhibit two expected cusps at 14 K and 213 K. However, such two cusps take place slight shifts compared with individual u-Fe_3O_4 (10 K) and Fe_3O_4/silica nanoparticles (231 K). The shift is probably due to the magnetic interaction between the u-Fe_3O_4 nanoparticles and Fe_3O_4 core. Specifically, such interaction is expected to induce an enhanced thermal field effect under an alternative electromagnetic field, forming uniform temperature gradient in the whole silica shell.

As one of the most widely used anticancer drugs, conjugating doxorubicin molecules in nanocarriers with controllable release has been attracting considerable attention due to its dose-dependent toxic side effects.[33] Herein we recently developed the chemical grafting protocol for constructing pH-dependent clickable linkers between the doxorubicin molecules and amine groups via 1,2-cyclohexanedicarboxylic anhydride.[1,5] Such amides are stable at neutral pH, but charged to regenerate the amine groups at low pH, accompanying with the release of the doxorubicin molecules. The loading and cumulative release were quantitatively evaluated by comparing the normalized absorbance intensity of characteristic peaks of doxorubicin molecules at 450~550 nm. The release profiles of doxorubicin molecules at 37 °C at pH 7.4 and 5.0 are shown in Fig. 5(a) and (b), respectively. At pH 7.4, the releasing process initially reached 4 % in 100 min, and then up to 600 min the whole release fractions was less than 8 % for both samples. The maximum loading of coupled doxorubicin molecules was about 4.1 and 1.2 mg for 100 mg Fe_3O_4/silica and Fe_3O_4/silica/u-Fe_3O_4 nanoparticles, while 98 % and 84 % of them can be effectively released at pH 5.0 and 37 °C for 600 min, respectively.

As an alternative, we herein further developed another route to remotely control the release of doxorubicin molecules using an external electromagnetic field. As is well known, magnetic particles can transform the energy of electromagnetic field to thermal form by magnetic hysteresis and eddy current losses, inducing the localized heating, which has been used as hyperthermia in tumor treatment. To exhibit the remote heating behavior, we measured the temperature-time relationship of 10 mg/ml DOX-nanoparticle/PBS suspensions under the electromagnetic irradiation of 400 kHz. The results showed that the temperature increases for two different samples rise up to 70 °C and 50 °C with 10 min, respectively, as shown in Figure 6(a). The temperature gradient in the whole silica shell is reasonably expected to be higher than that we observed and plays critical role in accelerating the diffusion and release of loaded DOX molecules. Figure 6(b) shows the DOX release curves of two kinds of nanoparticles triggered by the electromagnetic field irradiation at pH 7.4. The electromagnetic field was carried out for 10 min at each time point as indicated by arrows. One can find that a rapid response of release occurs at each triggered point, and reach 92 % release efficiency after 5 irradiation cycles at pH 7.4.

Moreover, the microstructures of DOX conjugated Fe_3O_4/silica/u-Fe_3O_4 nanoparticles was not changed, as shown in Figure 7(a),

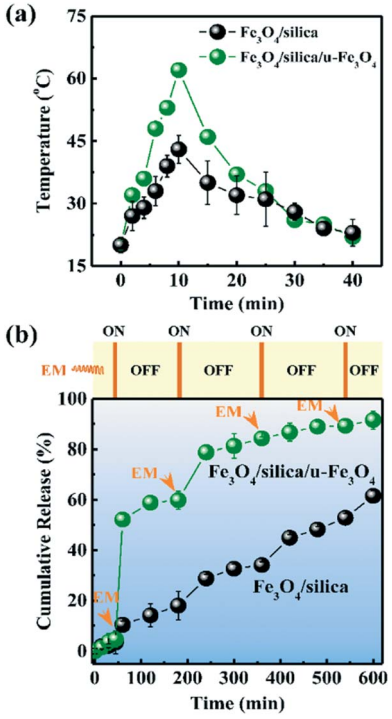

Fig. 6 DOX release curves of two kinds of nanoparticles, (a) temperature increase curves of Fe_3O_4/silica nanoparticles and DOX conjugated Fe_3O_4/silica/u-Fe_3O_4 nanoparticles under the irradiation of electromagnetic field for 10 min and the subsequently cooling process, (b) at pH 7.4 and under electromagnetic field irradiation (10 minutes at each point as indicated by arrows).

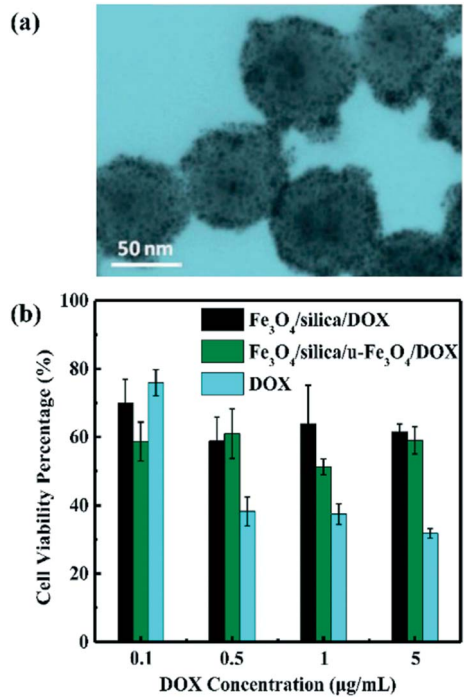

Fig. 7 (a) TEM image of DOX conjugated Fe_3O_4/silica/u-Fe_3O_4 nanoparticles after the electromagnetic triggered release. (b) Cell viability percentage after 48 hrs incubation with Fe_3O_4/silica nanoparticles and DOX conjugated Fe_3O_4/silica/u-Fe_3O_4 nanoparticles, and free DOX with various concentrations.

indicating that the u-Fe_3O_4 nanoparticles cannot be diffused into the circulation system during the drug release process. The cell viability of Fe_3O_4/silica/u-Fe_3O_4 nanoparticles conjugated with DOX was evaluated using A549 cells, adenocarcinomic human alveolar basal epithelial cells. After 48 h incubation, the MTT assay results indicate that the Fe_3O_4/silica and Fe_3O_4/silica/u-Fe_3O_4 nanoparticles are relatively non-toxic at concentrations of 0.1, 0.5, 1 and 5 μg/mL with around 60% cell viability, whereas free DOX exhibits a serious loss of cell viability, as shown in Figure 7(b).

4. Conclusions

We have demonstrated a proof-of-concept for the synthesis of pH and electromagnetic field dual-triggered drug release vehicle by decorating ultrathin Fe_3O_4 nanoparticles on the surface of Fe_3O_4/silica core/shell nanoparticles. This new magnetic architecture offer a properties required for drug delivery, meanwhile, providing the possibility to enhance the magnetic manipulation, hyperthermia, and magnetic imaging functions.

Acknowledgments

The authors gratefully acknowledge the National Natural Science Foundation of China (U1704253, 51471045, 51401049), the fundamental research funds for the central universities (N160208001), the national 1000-plan for young scholars and the start-up funding supported from the Northeastern University of China.

References

1 P. Xu, E. A. V. Kirk, Y. Zhan, W. J. Murdoch, M. Radosz and Y. Shen, *Angew. Chem., Int. Ed.*, 2007, **46**, 4999–5002.
2 W. Wu, T. Zhou, A. Berliner, P. Banerjee and S. Zhou, *Chem. Mater.*, 2010, **22**, 1966–1976.
3 E. Aznar, M. D. Marcos, R. Martínez-Máñez, F. Sancenón, J. Soto, P. Amorós and C. Guillem, *J. Am. Chem. Soc.*, 2009, **131**, 6833–6843.
4 F. H. Chen, L. M. Zhang, Q. T. Chen, Y. Zhang and Z. J. Zhang, *Chem. Commun.*, 2010, **46**, 8633–8635.
5 X. F. Zhang, S. Mansouri, L. Clime, H. Q. Ly, L 'H. Yahia and T. Veres, *J. Mater. Chem.*, 2012, **22**, 14450–14457.
6 J. Z. Du, X. J. Du, C. Q. Mao and J. Wang, *J. Am. Chem. Soc.*, 2011, **133**, 17560–17563.
7 E. Q. Song, W. E. Han, C. Li, D. Cheng, L. R. Li, L. C. Liu, G. Z. Zhu, Y. Song and W. H. Tan, *ACS Appl. Mater. Interfaces*, 2014, **6**, 11882–11890.
8 C. Y. Yang, W. Guo, L. R. Cui, N. An, T. Zhang, H. M. Lin and F. Qu, *Langmuir*, 2014, **30**, 9819–9827.
9 L. F. Chen, J. C. Di, C. Y. Cao, Y. Zhao, Y. Ma, J. Luo, Y. Wen, W. Song, Y. Song and L. Jiang, *Chem. Commun.*, 2011, **47**, 2850–2852.
10 J. Mikkila, A. P. Eskelinen, E. H. Niemela, V. Linko, M. J. Frilander, P. Torma and M. A. Kostiainen, *Nano Lett.*, 2014, **14**, 2196–2200.
11 K. Patel, S. Angelos, W. R. Dichtel, A. Coskun, Y. W. Yang, J. I. Zink and J. F. Stoddart, *J. Am. Chem. Soc.*, 2008, **130**, 2382–2383.
12 V. Raeesi, L. Y. T. Chou and W. C. W. Chan, *Adv. Mater.*, 2016, **28**, 8511–8518.
13 R. Liu, Y. L. Guo, G. Odusote, F. L. Qu and R. D. Priestley, *ACS Appl. Mater. Interfaces*, 2013, **5**, 9167–9171.
14 T. Darbre and J. L. Reymond, *Acc. Chem. Res.*, 2006, **39**, 925–934.
15 X. Wang, W. H. Chen, X. D. Xu, C. Li, J. Zhang, R. X. Zhuo and X. Zhang, *Adv. Mater.*, 2011, **23**, 3526–3530.
16 P. D. Thornton and A. Heise, *J. Am. Chem. Soc.*, 2010, **132**, 2024–2028.
17 T. D. Nguyen, K. C. F. Leung, M. Liong, Y. Liu, J. F. Stoddart and J. I. Zink, *Adv. Funct. Mater.*, 2007, **17**, 2101–2110.
18 B. P. Jia and L. Gao, *J. Phys. Chem. C.*, 2008, **112**, 666–671.
19 N. K. Mal, M. Fujiwara and Y. Tanaka, *Nature*, 2003, **421**, 350–353.
20 T. J. Yoon, J. S. Kim, B. G. Kim, K. N. Yu, M. H. Cho and J. K. Lee, *Angew. Chem., Int. Ed.*, 2005, **44**, 1068–1071.
21 S. Giri, B. G. Trewyn, M. P. Stellmaker and V. S. Y. Lin, *Angew. Chem., Int. Ed.*, 2005, **44**, 5038–5044.
22 Y. H. Li, N. Li, W. Pan, Z. Z. Yu, L. M. Yang and B. Tang, *ACS Appl. Mater. Interfaces*, 2017, **9**, 2123–2129.
23 Y. F. Zhu, T. Ikoma, N. Hanagata and S. Kaskel, *Small*, 2010, **6**, 471–478.
24 X. Li, X. P. Wang, Z. Hua and J. Shi, *Acta Materialia*, 2008, **56**, 3260–3265.
25 C. Liong, D. Ortiz, E. Ao-ieong, M. S. Navati, J. M. Friedman and P. Cabrales, *Nanotechnology*, 2014, **25**, 265102.
26 S. J. Son, J. Reichel, B. He, M. Schuchman and S. B. Lee, *J. Am. Chem. Soc.*, 2005, **127**, 7316–7317.
27 W. P. Li, P. Y. Liao, C. H. Su and C. S. Yeh, *J. Am. Chem. Soc.*, 2014, **136**, 10062–10075.
28 J. E. Lee, N. Lee, H. Kim, J. Kim, S. H. Choi, J. H. Kim, T. Kim, I. C. Song, S. P. Park, W. K. Moon and T. Hyeon, *J. Am. Chem. Soc.*, 2010, **132**, 552–557.
29 S. D. Kong, W. Zhang, J. H. Lee, K. Brammer, R. Lal, M. Karin and S. Jin, *Nano Lett.*, 2010, **10**, 5088–5092.
30 J. Zhang, Z. F. Yuan, Y. Wang, W. H. Chen, G. F. Luo, S. X. Cheng, R. X. Zhuo and X. Z. Zhang, *J. Am. Chem. Soc.*, 2013, **135**, 5068–5073.
31 C. Coll, A. Bernardos, R. Martínez-Máñez and F. Sancenón, *Acc. Chem. Res.*, 2013, **46**, 339–349.
32 H. Iida, K. Takayanagi, T. Nakanishi and T. Osaka, *J. Colloid Interf. Sci.*, 2007, **314.1**, 274–280.
33 D. L. Crowe, *Recent Res. Dev. Cancer*, 2002, **4**, 65–72.

